

Kalirin Promotes Neointimal Hyperplasia by Activating Rac in Smooth Muscle Cells

Jiao-Hui Wu, Alexander C. Fanaroff, Krishn C. Sharma, Liisa S. Smith, Leigh Brian, Betty A. Eipper, Richard E. Mains, Neil J. Freedman, Lisheng Zhang

Objective—Kalirin is a multifunctional protein that contains 2 guanine nucleotide exchange factor domains for the GTPases Rac1 and RhoA. Variants of *KALRN* have been associated with atherosclerosis in humans, but Kalirin's activity has been characterized almost exclusively in the CNS. We therefore tested the hypothesis that Kalirin functions as a Rho-guanine nucleotide exchange factor in arterial smooth muscle cells (SMCs).

Methods and Results—Kalirin-9 protein is expressed abundantly in aorta and bone marrow, as well as in cultured SMCs, endothelial cells, and macrophages. Moreover, arterial Kalirin was upregulated during early atherogenesis in apolipoprotein E-deficient mice. In cultured SMCs, signaling was affected similarly in 3 models of Kalirin loss-of-function: heterozygous *Kalrn* deletion, Kalirin RNAi, and treatment with the Kalirin Rho-guanine nucleotide exchange factor -1 inhibitor 1-(3-nitrophenyl)-1H-pyrrole-2,5-dione. With reduced Kalirin function, SMCs showed normal RhoA activation but diminished Rac1 activation, assessed as reduced Rac-GTP levels, p21-activated kinase autophosphorylation, and SMC migration. *Kalrn*^{-/-} SMCs proliferated 30% less rapidly than wild-type SMCs. Neointimal hyperplasia engendered by carotid endothelial denudation was ≈60% less in *Kalrn*^{-/-} and SMC-specific *Kalrn*^{-/-} mice than in control mice.

Conclusion—Kalirin functions as a guanine nucleotide exchange factor for Rac1 in SMCs, and promotes SMC migration and proliferation both in vitro and in vivo. (*Arterioscler Thromb Vasc Biol.* 2013;33:00-00.)

Key Words: guanine nucleotide exchange factors ■ neointimal hyperplasia ■ signal transduction ■ smooth muscle cells

Human atherosclerosis has been associated with variants of the gene *KALRN* in several independent human cohorts,¹⁻³ yet the function of the proteins encoded by *KALRN*—Kalirin isoforms—has been studied almost exclusively in neurons and pituitary cells. The most abundantly expressed Kalirin isoform outside the CNS is Kalirin-9, for which mRNA is detectable in aorta, liver, and skeletal muscle of adult mice.⁴ A 270-kDa protein, Kalirin-9 is one of only 2 mammalian proteins that contain 2 GDP/GTP exchange factors (GEFs) for the Rho family GTPases, which are critical for cytoskeletal dynamics and consequently for cell motility and proliferation.⁵ Phylogenetic conservation from *C. elegans* to human attests to the importance of Kalirin-9 in cell biology.⁶ Kalirin-9 comprises an N-terminal phospholipid-binding Sec14p domain followed by 9 spectrin repeats, its RhoGEF1 domain, a Src-homology 3 (SH3) domain, its RhoGEF2 domain, and a second SH3 domain (Figure 1A).⁶ Whereas the RhoGEF1 domain of Kalirin activates Rac1 and RhoG, the RhoGEF2 domain activates RhoA.⁶ The spectrin repeats are known thus far to bind to the N-terminal region of inducible nitric oxide synthase (NOS2),⁷ to peptidylglycine α -amidating monooxygenase, Huntingtin-associated

protein-1, Disrupted-in-Schizophrenia 1, Arf6, sorting nexins 1 and 2, and α II-spectrin.^{6,8} Kalirin has one mammalian ortholog, named Trio, with which Kalirin shares 65% to 85% amino acid identity in the RhoGEF domains.⁶ Nevertheless, Kalirin and Trio are not interchangeable: *Trio*^{-/-} and *Kalrn*^{-/-} mouse embryos die during development on the 129/C57BL/6 mixed genetic background,^{4,6} and *Kalrn*^{-/-} mice show diminished size and multiple abnormalities on the C57BL/6 background.⁴

Kalirin's RhoGEF activity could plausibly augment atherogenesis by enhancing vascular smooth muscle cell (SMC) proliferation and migration,⁹⁻¹¹ and endothelial dysfunction,¹² among other mechanisms. Of the 60 to 70 RhoGEFs encoded by mammalian genomes,¹³ 27 are expressed as mRNAs in SMCs,¹⁴ but only a third of these have been shown to serve unique functions in SMCs.¹⁴⁻¹⁹ By activating Rac1 in SMCs, Kalirin's RhoGEF1 activity could promote SMC migration and proliferation by activating the p21-activated (Ser/Thr) kinase (PAK),²⁰⁻²² and NADPH oxidases.²³ By activating RhoA, Kalirin's RhoGEF2 activity could promote not only SMC migration and proliferation,²⁴ but also endothelial dysfunction¹²—through the action of the Rho-associated coiled-coil-containing protein (Ser/

Received on: July 30, 2012; final version accepted on: December 11, 2012.

From the Departments of Medicine (Cardiology) (J.-H.W., A.C.F., K.C.S., L.S.S., L.B., N.J.F., L.Z.) and Cell Biology (N.J.F.), Duke University Medical Center, Durham, NC; and Department of Neuroscience, University of Connecticut Health Center, Farmington, CT (B.A.E., R.E.M.).

The online-only Data Supplement is available with this article at <http://atvb.ahajournals.org/lookup/suppl/doi:10.1161/ATVBAHA.112.300234/-/DC1>.

Correspondence to Neil J. Freedman or Richard E. Mains, Box 3187, Duke University Medical Center, Durham, NC 27710 or Department of Neuroscience, University of Connecticut Health Science Center, Farmington CT 06030. E-mail neil.freedman@duke.edu or mains@uchc.edu

© 2013 American Heart Association, Inc.

Arterioscler Thromb Vasc Biol is available at <http://atvb.ahajournals.org>

DOI: 10.1161/ATVBAHA.112.300234

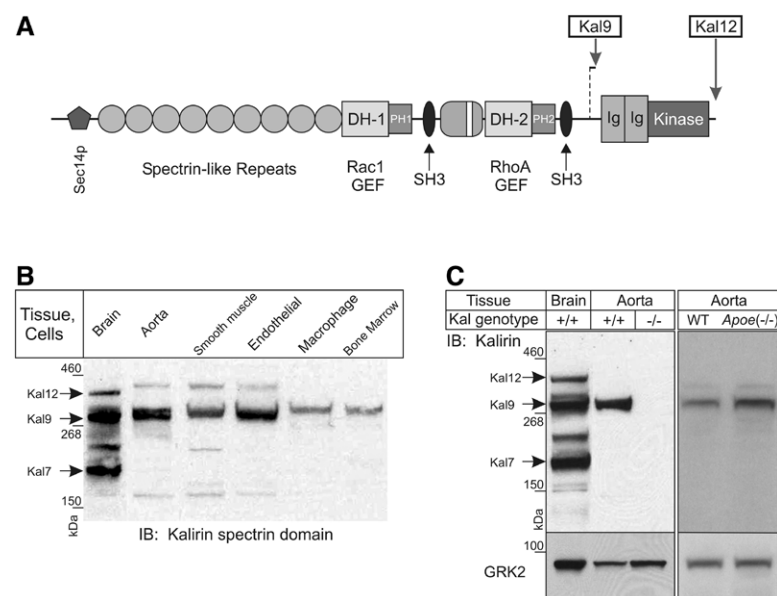


Figure 1. Vascular and bone marrow-derived cells express Kalirin-9, which is upregulated during atherogenesis. **A**, A scale drawing of the domain topography of Kalirins -9 and -12 (named for the size of their mRNA). DH-1 indicates Dbl (deleted in B-cell lymphoma) homology-1; Ig, immunoglobulin; Kinase, Ser/Thr kinase; PH, pleckstrin homology; Sec14p, phospholipid-binding; and SH3, Src homology 3. **B**, The indicated tissues and primary cell lines from wild-type (WT) mice were solubilized; 35 μ g protein was subjected to SDS-PAGE and immunoblotted with anti (Kalirin spectrin domain)-IgG. Parallel blots probed with nonimmune first IgG yielded no bands (not shown). **Arrows** indicate Kalirin isoforms. Shown is a single experiment, representative of 3 performed. **C**, Mice of the indicated genotype were euthanized; 35 μ g of tissue was immunoblotted for Kalirin, as in panel **B**. The nitrocellulose was stripped and reprobed for G protein-coupled receptor kinase-2 (GRK2) as a loading control. Shown are immunoblots representative of 3 independent experiments.

Thr) kinases. We sought to test the hypothesis that Kalirin-9 functions as a dual Rho-GEF in SMCs, and thereby promotes SMC activation in vitro and in vivo. To do so, we used primary aortic SMCs from wild-type (WT) and congenic *Kalrn*^{-/-} mice, as well as wire-mediated carotid endothelial denudation injury in WT and congenic *Kalrn*^{-/-} mice.

Materials and Methods

For complete Methods, see online-only Data Supplement.

Mice

All mice were congenic on the C57BL/6 background (≥ 10 generations back-crossed). The Kalirin spectrin repeat knockout mouse was created as described;⁴ *Kalrn*^{-/-} and littermate WT mice were created from matings of *Kalrn*^{-/-} mice, which appeared phenotypically indistinguishable from WT mice. SMC-specific *Kalrn*^{-/-} mice were created by mating *Kalrn*^{fllox/+} with SM22 α -Cre mice (Jackson Laboratory stock #004746), to obtain SM22 α -Cre⁺/*Kalrn*^{fllox/+} (SMC-*Kalrn*^{-/-}) mice.

Cell Culture and Assays

Mouse aortic SMCs were isolated by enzymatic digestion of aortas and passaged as described.^{9,25} SMC proliferation and migration studies as well as immunoblotting assays were performed as described.⁹ We previously developed rabbit polyclonal antibodies against the spectrin domain of Kalirin²⁶ and Trio.²⁷ Determinations of RhoA-GTP and Rac1-GTP levels, respectively, were made with RhoA and Rac1 G-LISAs (Cytoskeleton, Inc).

Mouse Surgeries

Wire-mediated endothelial denudation of the common carotid^{9,28} was performed as described.

Results

Vascular Expression of Kalirin

To delineate potential loci of Kalirin activity in vascular biology, we first immunoblotted mouse tissues and cells to determine their Kalirin-expression levels relative to those obtained

in mouse brain. As Figure 1B shows, primary SMCs, endothelial cells, and macrophages all express Kalirin-9 at levels comparable with those obtained from mouse brain, and similar findings were obtained by using extracts from mouse aorta or bone marrow. In contrast, aortas from *Kalrn*^{-/-} mice demonstrated no immunoreactivity corresponding to Kalirin-9 (Figure 1C). To determine whether Kalirin expression changed in the context of atherogenesis, we compared thoracic aortas from WT and *Apoe*^{-/-} mice aged 8 weeks, before intimal macrophage infiltration occurs.²⁹ Kalirin-9 protein expression was 1.6 \pm 0.2-fold higher in aortas from *Apoe*^{-/-} than from WT mice ($P<0.05$; Figure 1C). Thus, vascular cell expression of Kalirin-9 is upregulated during the earliest stages of atherogenesis.

Kalirin Activates Rac1 in SMCs

To test whether Kalirin function affects SMC physiology, we first inhibited Kalirin's RhoGEF1 domain by treating primary SMCs with the cell-permeant compound NPPD (1-(3-nitrophenyl)-1H-pyrrole-2,5-dione), which selectively inhibits GDP/GTP exchange activity promoted by the highly homologous RhoGEF1 domains of Kalirin and its lone ortholog, Trio.³⁰ Kalirin's RhoGEF1 and RhoGEF2 domains activate Rac1 and RhoA, respectively (Figure 1A).⁶ We therefore assessed SMC Rac1 and RhoA activity, by determining the activity of their respective effector kinases: PAK1, which when activated by Rac1-GTP autophosphorylates on Thr-423;³¹ and Rho-associated coiled-coil-containing protein kinases (ROCK1, ROCK2), which when activated by RhoA-GTP phosphorylate the myosin phosphatase-targeting subunit 1 (MYPT1) on Thr-853.³² PAK1 autophosphorylation induced by platelet-derived growth factor (PDGF) was reduced by 40 \pm 20% ($P<0.05$) in SMCs treated with NPPD (Figure 2A and 2B). In contrast, (ROCK-mediated) MYPT1 phosphorylation was not affected by NPPD (Figure 2A and 2B). Thus, the RhoGEF1 domain of Kalirin or Trio—known to activate Rac1, but not RhoA⁶—appears to mediate Rac1 activation downstream of the PDGF receptor in SMCs. To distinguish Kalirin from Trio

in this NPPD-sensitive SMC Rac1 activation, we compared Kalirin and Trio expression in SMCs with that in brain tissue, in which Trio and Kalirin are expressed at comparable levels (quantitative real-time PCR data not shown). Whereas SMC Trio protein levels were <5% of brain levels, SMC Kalirin protein levels were comparable with those in brain tissue (Figure 2C). Consequently, we inferred that most of the NPPD-inhibited, PDGF-induced Rac-GEF activity in SMCs is attributable to Kalirin, rather than to Trio.

To complement NPPD-mediated inhibition of Kalirin's RhoGEF1 domain, and to determine whether Kalirin's

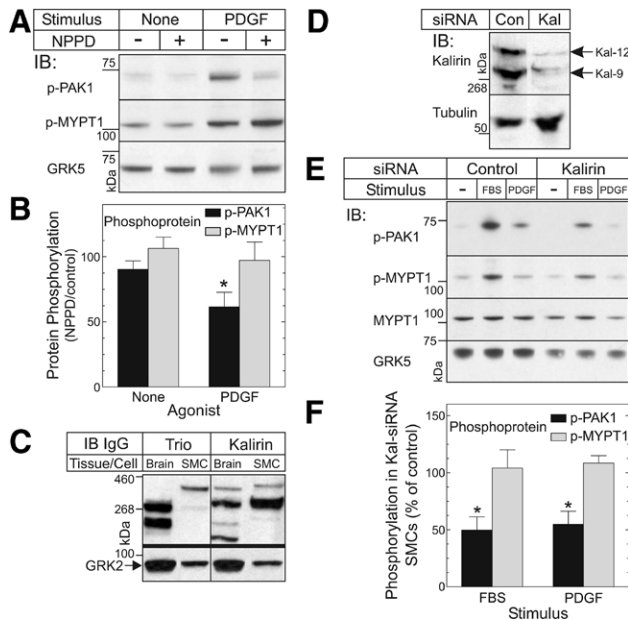


Figure 2. Smooth muscle cell (SMC) Kalirin activates Rac1, but not RhoA: inhibitor and RNAi data. **A**, Quiescent aortic SMCs were treated for 2.5 hours with 0.1% dimethyl sulfoxide (DMSO) lacking (control) or containing the Kalirin RhoGEF1 domain inhibitor NPPD (1-(3-nitrophenyl)-1*H*-pyrrole-2,5-dione; 100 μ Mol/L [final]). Subsequently, SMCs were exposed to serum-free medium lacking (None) or containing 1 nmol/L platelet-derived growth factor (PDGF)-BB (10 minutes, 37°C), solubilized, and immunoblotted for phospho- (p-) p21-activated (Ser/Thr) kinase (PAK) 1 (p-Thr423), p-myosin phosphatase-targeting subunit 1 (MYPT1; p-Thr853), and then for G protein-coupled receptor kinase-5 (GRK5; as a loading control). **B**, The indicated phosphoprotein band densities were normalized to cognate GRK5 bands on each blot; quotients were divided by those obtained from control-treated SMCs within each experiment to obtain percentage of control, plotted as means \pm SE of 3 experiments. Compared with control: *indicates $P<0.05$. **C**, Protein extracts (35 μ g/lane) of whole mouse brain and SMCs were immunoblotted with IgG specific for Trio or Kalirin, and then reprobed for GRK2 (as a loading control). Results are from a single experiment representative of 3 performed. **D**, SMCs transfected with small interfering RNA targeting no known protein (control, Con) or Kalirin (Kal) were immunoblotted for Kalirin and then tubulin; the mobility of Kalirin isoforms is indicated by arrows. Results shown are from a single experiment representative of 3 performed. **E**, SMCs from panel **D** were exposed to medium lacking or containing 10% FBS or 1 nmol/L PDGF-BB (10 minutes, 37°C), and then processed for immunoblotting, as in panel **A**. **F**, The indicated phosphoprotein band densities were normalized to cognate GRK5 bands on each blot; quotients from Kal-siRNA transfected SMCs were divided by those obtained from control small interfering RNA-transfected SMCs within each experiment to obtain percentage of control, plotted as means \pm SE of 3 experiments. Compared with control: * $P<0.05$.

RhoGEF2 domain is also important in SMC physiology, we used Kalirin RNAi. Relative to SMCs transfected with control small interfering RNA, SMCs transfected with Kalirin-targeting small interfering RNA demonstrated 43 \pm 9% less Kalirin protein expression and 50 \pm 20% less PAK1 autophosphorylation in response to PDGF or serum ($P<0.05$; Figure 2D–2F). Nevertheless, Kalirin knockdown SMCs demonstrated MYPT1 phosphorylation (evidence of ROCK activity)³² that was equivalent to control SMCs (Figure 2E and 2F). Thus, we obtained equivalent results in SMCs with Kalirin knockdown and chemical inhibition of Kalirin's RhoGEF1 domain, and Kalirin appears to function in SMCs as an important GEF for Rac1, but not for RhoA.

To corroborate these data obtained with Kalirin RNAi, we used 5 independently isolated lines of SMCs from age- and sex-matched *Kalrn*^{-/-} and littermate WT mice. *Kalrn*^{-/-} SMCs expressed only 45 \pm 5% as much Kalirin-9 protein as WT SMCs, but equivalent levels of proteins critical for the receptor tyrosine kinase and (heterotrimeric) G_{q/11} signal transduction pathways under investigation: PDGF receptor- β , endothelin receptor type A, Rac1, RhoA, PAK1, and MYPT1 (Figure 3A). When stimulated with serum, PDGF, or endothelin-1, *Kalrn*^{-/-} SMCs demonstrated only \approx 60% of WT PAK1 activation, as assessed by PAK1 autophosphorylation (Figure 3B and 3C). In contrast, *Kalrn*^{-/-} SMCs demonstrated WT levels of ROCK activation, as assessed by MYPT1 phosphorylation³² (Figure 3B and 3C). Because ROCK isoforms can be activated not only by RhoA (the target of Kalirin's RhoGEF2 domain), but also by RhoB and RhoC,³³ we also assessed SMC RhoA-GTP levels. Consistent with MYPT1 phosphorylation data, *Kalrn*^{-/-} and WT SMCs demonstrated equivalent, 2- to 3-fold over basal stimulation of RhoA-GTP loading in response to serum (Figure 3D). In contrast, *Kalrn*^{-/-} SMCs demonstrated 30% less Rac1-GTP loading than WT SMCs (Figure 3D). Thus, assessed at the level of the GTPase or the effector kinases, Kalirin appears to promote the activation of Rac1, but not RhoA, in SMCs.

Kalirin Promotes SMC Migration and Proliferation

Because Rac1 and PAK1 signaling are critical for SMC migration,^{20,21} we reasoned in light of Figure 3 that loss of Kalirin function would reduce SMC migration. To test this hypothesis, we studied SMC migration in modified Boyden chambers. Stimulus-independent SMC migration was not affected by loss of Kalirin function (Figure 4). However, whether engendered by chemical inhibition of Kalirin's RhoGEF1 domain (by NPPD), by Kalirin RNAi, or by Kalirin haploinsufficiency, loss of Kalirin function was associated with a \approx 35% reduction in PDGF- or serum-evoked SMC migration ($P<0.05$; Figure 4). To determine whether loss of Kalirin function reduced SMC migration principally by reducing Rac1 activation, we treated SMCs with the cell-permeant Kalirin RhoGEF1 inhibitor ITX3³⁴ or the Rac1 inhibitor Z62954982, using conditions that have been shown to inhibit PDGF-induced GTP loading of Rac1 by \approx 50% without affecting GTP loading of the related Rho-GTPases Cdc42 or RhoA.³⁵ Kalirin RhoGEF1 or Rac1 inhibition with ITX3 or Z62954982, respectively, reduced by 35% to 40% the migration of WT SMCs stimulated by PDGF (Figure 4D). This attenuation of SMC migration was

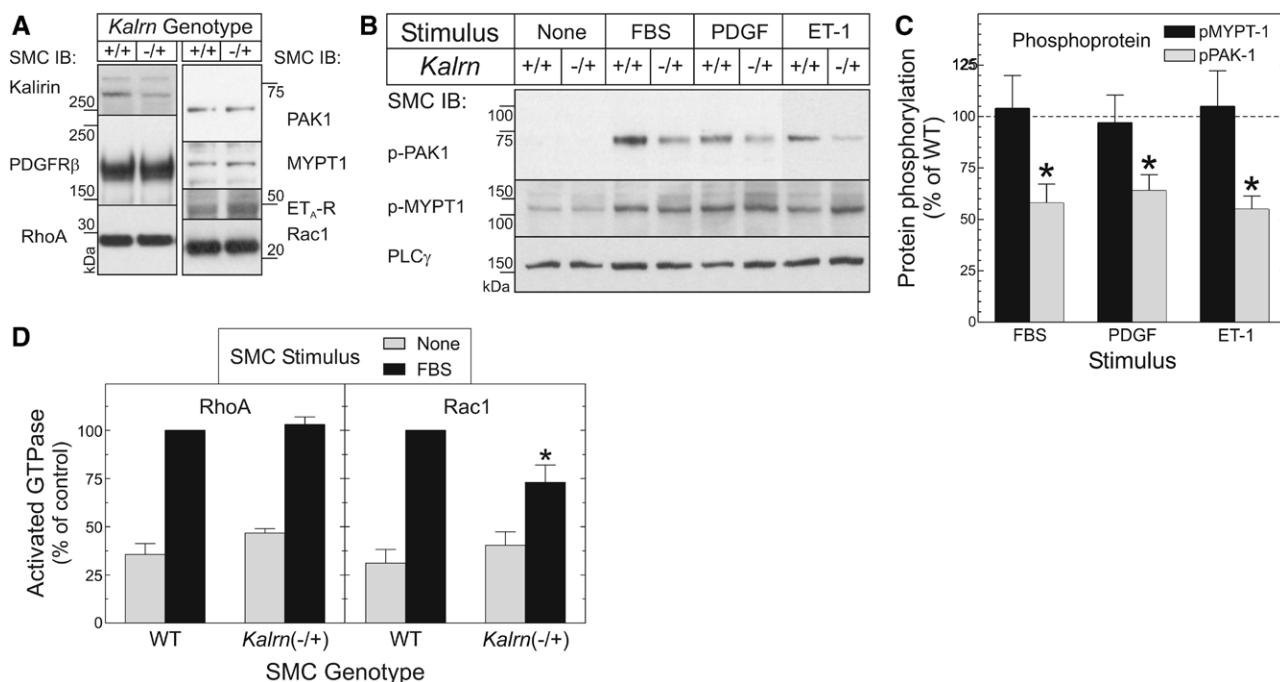


Figure 3. Smooth muscle cell (SMC) Kalirin activates Rac1, but not RhoA: data from *Kalrn*^{-/-} and wild-type (WT) SMCs. **A**, Solubilized extracts (40 μ g protein/lane) from WT (*Kalrn*^{+/+}) and *Kalrn*^{-/-} SMCs were immunoblotted serially for the indicated proteins: platelet-derived growth factor receptor β (PDGFR β), PDGFR β ; ET_A-R, endothelin receptor type A. Shown are results from a single experiment representative of 5 performed. **B**, Quiescent SMCs from WT or *Kalrn*^{-/-} mice were exposed for 10 minutes (37°C) to serum-free medium lacking (None) or containing 10% FBS, 2 nmol/L PDGF-BB, or 100 nmol/L endothelin-1 (ET-1), then solubilized and immunoblotted for the indicated (phospho) proteins. PLC γ (phospholipase C- γ) was used as a loading control. Shown are results from a single experiment, representative of 5 performed. **C**, The indicated phosphoprotein band densities were normalized to cognate PLC γ bands; quotients were divided by those of WT SMCs to obtain percentage of WT, plotted as means \pm SE of 5 experiments with independently isolated WT and *Kalrn*^{-/-} SMC lines. Compared with WT: *indicates $P < 0.05$. **D**, Quiescent WT and *Kalrn*^{-/-} SMCs were stimulated as in panel B, lysed, and subjected to RhoA or Rac1 G-LISA (Cytoskeleton, Inc). Absorbance values were normalized in each experiment to the value obtained for FBS-stimulated WT SMCs, to obtain percentage of control. Shown are the means \pm SE from ≥ 3 experiments performed in triplicate. Compared with WT: * $P < 0.05$.

comparable with that seen with the loss of Kalirin function observed in *Kalrn*^{-/-} SMCs. Furthermore, the impaired migration of *Kalrn*^{-/-} SMCs was not further reduced by ITX3 or Z62954982 (Figure 4D). In parallel experiments with WT SMCs, Z62954982 inhibited PAK1 autophosphorylation by 40 \pm 10%, but neither ITX3 nor Z62954982 inhibited ROCK activity, manifest as MYPT1 phosphorylation, or MEK1 activation, manifest as phosphorylation of ERK1/2 (Figure 4E and data not shown). As a further demonstration of inhibitor specificity, neither ITX3 nor Z62954982 reduced the SMC migration promoted by fetal bovine serum under the conditions prevailing in these experiments (Figure 4D). Taken together, these data suggest that Kalirin mediates Rac1 activation in SMCs downstream of the PDGF receptor, and thereby promotes SMC migration.

Whereas cellular migration can be promoted by Rac1 activity at the plasma membrane,²⁰ cellular proliferation appears to require Rac1 nuclear localization.³⁶ Thus, despite the observation that Kalirin promoted Rac1-dependent SMC migration, the effects of Kalirin on SMC proliferation remained uncertain. To test whether Kalirin activity promotes SMC proliferation, therefore, we quantitated WT and *Kalrn*^{-/-} SMCs at several time points during exposure to serum. *Kalrn*^{-/-} SMCs proliferated 50% less rapidly than WT SMCs in response to serum ($P < 0.03$; Figure 5). Thus, Kalirin appears to promote SMC proliferation.

SMC Kalirin Promotes Neointimal Hyperplasia

SMC proliferation and migration are fundamental to the neointimal hyperplasia that develops in response to arterial endothelial denudation.²⁸ If Kalirin's positive effects on SMC migration and proliferation occurred not only in vitro, but also in vivo, we reasoned that *Kalrn*^{-/-} mice should develop less neointimal hyperplasia than WT mice. We therefore provoked carotid artery neointimal hyperplasia in congenic *Kalrn*^{-/-} and WT mice by denuding the endothelium with a 0.36-mm wire—an approach that we have shown engenders neointimal hyperplasia comprising only SMCs from the arterial media.²⁸ Neointimal SMCs (Figure I in the online-only Data Supplement) demonstrated Kalirin upregulation (Figure II in the online-only Data Supplement). Congruent with our SMC studies (Figures 3 and 5), there was greater SMC PAK activation and proliferation in WT than in *Kalrn*^{-/-} arteries (Figures III and IV in the online-only Data Supplement); nonetheless, arterial reendothelialization, macrophage recruitment, and collagen content were equivalent in WT and *Kalrn*^{-/-} arteries (Figures V and VI in the online-only Data Supplement).

Kalrn^{-/-} mice developed 60% less neointima than WT mice (Figure 6 and Figure I in the online-only Data Supplement). However, this result could have been produced by pleiotropic effects of Kalirin in endothelial cells or leukocytes.³⁷ We therefore sought to ascertain that SMC Kalirin activity, specifically, was promoting the in vivo SMC proliferation

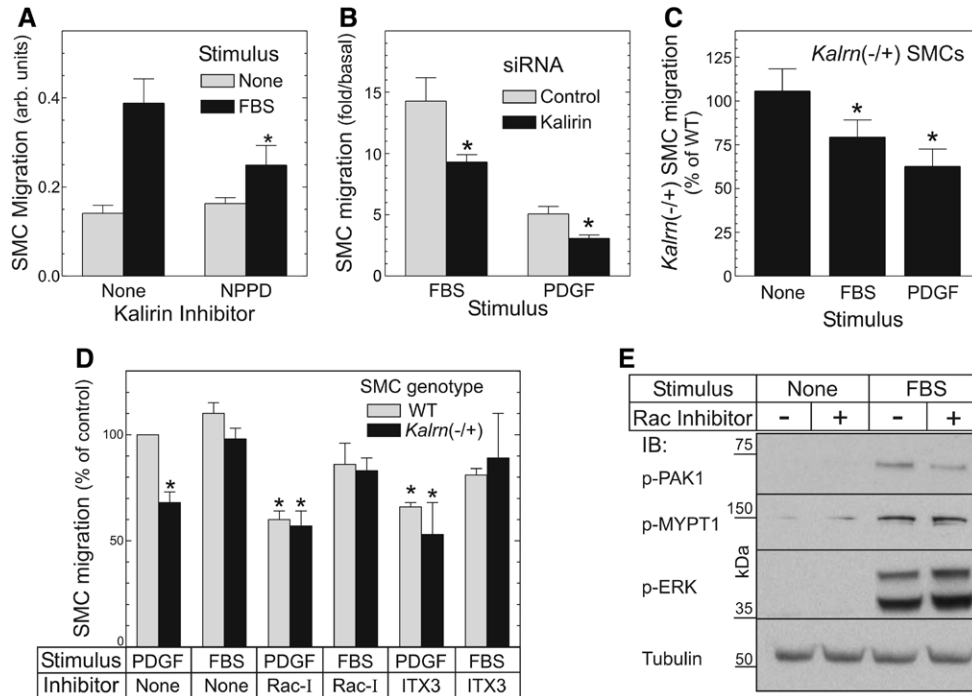


Figure 4. Kalirin promotes smooth muscle cell (SMC) migration. Quiescent SMCs in modified Boyden chambers were exposed to vehicle (basal), 10% FBS, or 1 nmol/L platelet-derived growth factor (PDGF)-BB; migrated SMCs were quantified colorimetrically (see Materials and Methods), and plotted as means \pm SE of ≥ 3 experiments performed in triplicate: as arbitrary (arb.) units (**A**), normalized to unstimulated SMC values (**B**), or normalized to cognate wild-type (WT) SMC values (**C**). Compared with control or WT: *indicates $P < 0.05$. **A**, WT SMCs were treated for 1 hour before migration assays with 0.1% dimethyl sulfoxide (DMSO) lacking (None) or containing the Kalirin RhoGEF1 inhibitor NPPD (1-(3-nitrophenyl)-1H-pyrrole-2,5-dione; 100 μ M/L). **B**, WT SMCs were transfected with the indicated small interfering RNA, and subjected to migration assay 72 hours later. Values for basal migration in Kalirin knockdown SMCs were $95 \pm 8\%$ of control SMC values. **C**, WT and *Kalrn*^{-/+} SMCs were subjected to migration assays in parallel. **D**, WT and *Kalrn*^{-/+} SMCs were exposed to 0.1% DMSO in serum-free medium lacking (None) or containing the Rac1 inhibitor (Rac-I) Z62954982 (10 μ M/L) or the Kalirin RhoGEF1 inhibitor ITX3 (100 μ M/L) for 4 hours before stimulation for migration assay. All migration values were normalized to those obtained for WT SMCs stimulated with 10% FBS, to obtain percentage of control. Values for basal migration in *Kalrn*^{-/+} SMCs were $100 \pm 10\%$ of WT values. Compared with vehicle-treated WT SMCs: *indicates $P < 0.05$. **E**, Quiescent WT SMCs were pretreated with vehicle or the Rac1 inhibitor as in panel **D**, challenged $\pm 10\%$ FBS (10 minutes, 37°C), and then processed for IB as in Figure 3. Shown are results from a single experiment, representative of ≥ 3 performed.

and migration of neointimal hyperplasia. To do so, we used mice with SMC-specific deletion of *Kalrn* (SMC-*Kalrn*^{-/-}, or SM22 α -Cre⁺/*Kalrn*^{lox/+}), and compared them with *Kalrn*^{lox/+} control mice (which gave results equivalent to WT mice [data not shown]). Compared with WT or *Kalrn*^{lox/+} control mice, SMC-*Kalrn*^{-/-} mice expressed Kalirin-9 protein levels that were $50 \pm 5\%$ less in endothelium-stripped aortas, but equivalent in whole-brain extracts (Figure 6A). After carotid endothelial denudation, SMC-*Kalrn*^{-/-} mice developed 65% less neointimal hyperplasia than in either control mouse cohort (Figure 6B and 6C). Before surgery, *Kalrn*^{-/-}, SMC-*Kalrn*^{-/-}, and WT mice had equivalent carotid dimensions (data not shown) and equivalent systolic blood pressures and heart rates: respectively, 121 ± 7 , 120 ± 10 , and 120 ± 10 mm Hg; 700 ± 40 , 640 ± 40 , and 660 ± 40 bpm ($n = 7/\text{group}$). Thus, whether in SMCs alone or in combination with endothelial cells and leukocytes, Kalirin activity contributes to neointimal hyperplasia.

Discussion

This study establishes Kalirin, a human atherosclerosis candidate gene,¹⁻³ as a significant signaling intermediate that promotes SMC Rac1 activation, migration, and proliferation downstream of the PDGF receptor- β and G protein-coupled

receptors in vitro (Figure VII in the online-only Data Supplement). Consonant with this signaling activity in SMCs, Kalirin in vivo promotes neointimal hyperplasia induced by arterial endothelial denudation—whether Kalirin expression is manipulated globally, or just in SMCs. It is noteworthy that Kalirin's role in vascular biology manifests with loss-of-function models that allow $\approx 50\%$ of normal Kalirin activity. Consequently, the magnitude of Kalirin's total contribution to vascular pathophysiology may be underestimated by these models; nevertheless, incomplete loss-of-function models human disease and pharmacotherapeutic responses better than complete loss-of-function.¹⁻³

Kalirin-promoted SMC migration and proliferation correlate with Kalirin's Rac1-GEF activity, triggered by the PDGF receptor- β : indeed, Kalirin deficiency impaired SMC migration only when Rac1 activity was intact (Figure 4). In neurons, Kalirin Rac-GEF activity is triggered by the receptor tyrosine kinase EphB2, which tyrosine-phosphorylates and recruits Kalirin to the plasma membrane.³⁸ Whether this method of Kalirin activation occurs downstream of the PDGF receptor- β tyrosine kinase remains to be established. However, SMCs express both EphB2 and its agonist ephrinB2, which appear to promote SMC migration in vivo;³⁹ thus, Kalirin could mediate SMC migration in vivo downstream of multiple receptor

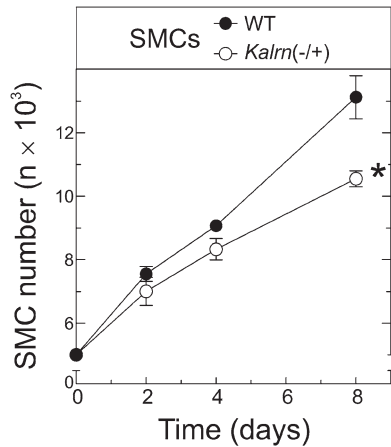


Figure 5. Kalirin increases smooth muscle cell (SMC) proliferation. Wild-type (WT) and *Kalrn*^{-/-} SMCs were incubated for indicated times in 10% FBS/growth medium; SMC quantification was performed as in section Materials and Methods. Plotted are the means±SE of SMC counts from 3 independent experiments with 3 independently isolated pairs of WT and *Kalrn*^{-/-} SMC lines. Compared with the WT growth curve: *indicates $P < 0.001$. The rate of SMC proliferation was obtained from linear regression ($R^2 = 0.98$ – 0.99).

tyrosine kinases. Furthermore, because EphB2 receptors on monocytes promote adhesion to arteries and because monocyte/macrophages express abundant Kalirin (Figure 1), it is conceivable that an EphB2–Kalirin signaling axis operates in monocytes to promote monocyte/macrophage infiltration of the (ephrinB2-expressing)³⁹ tunica media of injured arteries. Because monocyte/macrophages contribute significantly to neointimal hyperplasia,⁴⁰ Kalirin deficiency in monocytes could thus contribute to the reduction in neointimal hyperplasia we observed in *Kalrn*^{-/-} as compared with WT mice (Figure 6).

Despite containing a GEF domain specific for Rac1 and a GEF domain specific for RhoA,⁶ Kalirin appears to function in SMCs as a GEF only for Rac1, and not for RhoA. This inference is based on comparisons among SMCs with Kalirin levels that were either 100% or ~50% of WT; consequently, it may be that 50% of normal Kalirin levels in SMCs suffice to drive normal activation of RhoA, but not Rac1. Alternatively, Kalirin's apparent Rho-family GTPase specificity in SMCs may result from distinct subcellular distributions, and overlapping functions of the myriad Rac1- and RhoA-GEFs expressed along with Kalirin in SMCs.^{14–19} Lastly, it is important to note that the overall GTPase activity reflects a balance between the activities of GEFs, which activate GTPases by promoting the exchange of GTP for GDP, and GTPase-activating proteins, which deactivate GTPases by enhancing hydrolysis of GTP to GDP.⁵ Thus, it may be that the functionality of GTPase-activating proteins for Rac1 exceeds that of GTPase-activating proteins for RhoA in SMCs; if so, we could ascertain differences in Kalirin-mediated activation of Rac1 more sensitively than we could for RhoA.

Kalirin may also contribute to neointimal hyperplasia through mechanisms distinct from its Rac1-GEF activity. For example, Kalirin's interaction with the N-terminal domain of NOS2 prevents NOS2 dimerization, and thereby inhibits NOS2 activity.⁷ Perhaps because NOS2-produced NO reduces SMC proliferation and mitochondrial respiration,⁴¹ *Nos2*^{-/-} mice develop more medial thickening than WT mice

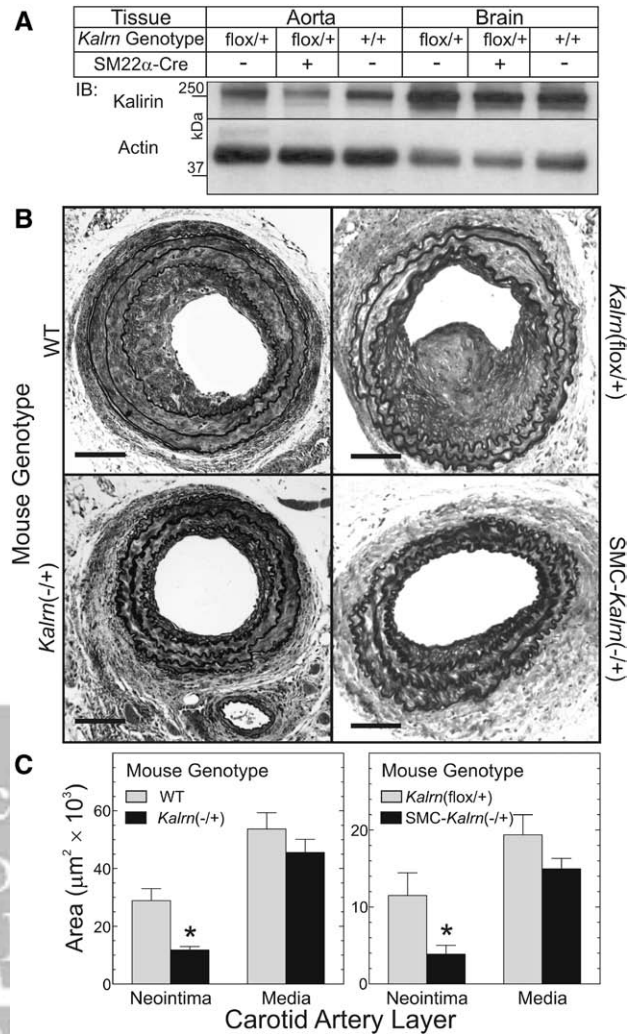


Figure 6. Smooth muscle cell (SMC) Kalirin promotes neointimal hyperplasia. **A**, Brains and aortas harvested from mice of the indicated genotype were solubilized and immunoblotted (40 μg protein/lane) serially for Kalirin and actin. Shown are results from a single experiment representative of 3 performed with independent mice. The ratio of Kalirin/actin was used for quantitation. **B**, Mice of the indicated genotype were subjected to carotid artery de-endothelialization and euthanized 4 weeks later. Perfusion-fixed carotids were stained with a modified connective tissue stain. Samples shown represent ≥5 of each genotype. Scale bars=50 μm. **C**, Cross-sectional areas for neointima and media are presented as means±SE from ≥5 carotids of each genotype. Compared with wild-type (WT): *indicates $P < 0.02$. Uninjured *Kalrn*^{-/-} and WT carotid arteries demonstrated equivalent lumen and medial areas (not shown).

subjected to carotid endothelial denudation.⁴² Consequently, by inhibiting SMC NOS2, Kalirin could reduce NO--mediated inhibition of SMC proliferation—and thereby contribute to neointimal hyperplasia. Whether such a mechanism occurs in SMCs remain to be established.

Achieved either genetically or by RNAi, just a 50% reduction in Kalirin activity suffices to reduce SMC proliferation and migration in vitro and in vivo. Consequently, Kalirin appears to be an appealing target for pharmacotherapy in SMC-proliferative disorders like neointimal hyperplasia. Because interventions that diminish neointimal hyperplasia often diminish atherosclerosis, too,^{28,43} the work presented

here adds credence to human genetic data^{1–3} implicating Kalirin in atherogenesis. Direct evidence to support Kalirin's role in atherosclerosis, of course, has yet to manifest.

Sources of Funding

This work was supported by NIH grants HL77185 and HL73005 (N.J.F.), DK32948 (B.A.E., R.E.M.), a Howard Hughes Medical Institute Medical Student Fellowship (A.C.F.), and an American Heart Association Grant-in-Aid (L.Z.).

Disclosures

None.

References

- Wang L, Hauser ER, Shah SH, et al. Peakwide mapping on chromosome 3q13 identifies the kalirin gene as a novel candidate gene for coronary artery disease. *Am J Hum Genet*. 2007;80:650–663.
- Krug T, Manso H, Gouveia L, et al. Kalirin: a novel genetic risk factor for ischemic stroke. *Hum Genet*. 2010;127:513–523.
- Ikram MA, Seshadri S, Bis JC, et al. Genomewide association studies of stroke. *N Engl J Med*. 2009;360:1718–1728.
- Mandela P, Yankova M, Conti LH, Ma X, Grady J, Eipper BA, Mains RE. Kalrn plays key roles within and outside of the nervous system. *BMC Neurosci*. 2012;13:136.
- Burridge K, Wennerberg K. Rho and Rac take center stage. *Cell*. 2004;116:167–179.
- Rabiner CA, Mains RE, Eipper BA. Kalirin: a dual Rho guanine nucleotide exchange factor that is so much more than the sum of its many parts. *Neuroscientist*. 2005;11:148–160.
- Ratovitski EA, Alam MR, Quick RA, McMillan A, Bao C, Kozlovsky C, Hand TA, Johnson RC, Mains RE, Eipper BA, Lowenstein CJ. Kalirin inhibition of inducible nitric-oxide synthase. *J Biol Chem*. 1999;274:993–999.
- Vishwanatha KS, Wang YP, Keutmann HT, Mains RE, Eipper BA. Structural organization of the nine spectrin repeats of Kalirin. *Biochemistry*. 2012;51:5663–5673.
- Wu JH, Zhang L, Fanaroff AC, Cai X, Sharma KC, Brian L, Exum ST, Shenoy SK, Peppel K, Freedman NJ. G protein-coupled receptor kinase-5 attenuates atherosclerosis by regulating receptor tyrosine kinases and 7-transmembrane receptors. *Arterioscler Thromb Vasc Biol*. 2012;32:308–316.
- Boucher P, Gotthardt M, Li WP, Anderson RG, Herz J. LRP: role in vascular wall integrity and protection from atherosclerosis. *Science*. 2003;300:329–332.
- Subramanian V, Golledge J, Ijaz T, Bruemmer D, Daugherty A. Pioglitazone-induced reductions in atherosclerosis occur via smooth muscle cell-specific interaction with PPAR[gamma]. *Circ Res*. 2010;107:953–958.
- Nohria A, Grunert ME, Rikitake Y, Noma K, Prsic A, Ganz P, Liao JK, Creager MA. Rho kinase inhibition improves endothelial function in human subjects with coronary artery disease. *Circ Res*. 2006;99:1426–1432.
- Kiraly DD, Eipper-Mains JE, Mains RE, Eipper BA. Synaptic plasticity, a symphony in GEF. *ACS Chem Neurosci*. 2010;1:348–365.
- Toumaniantz G, Ferland-McCollough D, Cario-Toumaniantz C, Pacaud P, Loirand G. The Rho protein exchange factor Vav3 regulates vascular smooth muscle cell proliferation and migration. *Cardiovasc Res*. 2010;86:131–140.
- Thill R, Campbell WB, Williams CL. Identification and characterization of the unique guanine nucleotide exchange factor, SmgGDS, in vascular smooth muscle cells. *J Cell Biochem*. 2008;104:1760–1770.
- Guilluy C, Brégeon J, Toumaniantz G, Rolli-Derkinderen M, Retailliau K, Loufrani L, Henrion D, Scalbert E, Bril A, Torres RM, Offermanns S, Pacaud P, Loirand G. The Rho exchange factor Arhgef1 mediates the effects of angiotensin II on vascular tone and blood pressure. *Nat Med*. 2010;16:183–190.
- Sakata Y, Xiang F, Chen Z, Kiriya Y, Kamei CN, Simon DI, Chin MT. Transcription factor CHF1/Hey2 regulates neointimal formation *in vivo* and vascular smooth muscle proliferation and migration *in vitro*. *Arterioscler Thromb Vasc Biol*. 2004;24:2069–2074.
- Shin EY, Lee CS, Park MH, Kim DJ, Kwak SJ, Kim EG. Involvement of betaPIX in angiotensin II-induced migration of vascular smooth muscle cells. *Exp Mol Med*. 2009;41:387–396.
- Fernstrom K, Farmer P, Ali MS. Cytoskeletal remodeling in vascular smooth muscle cells in response to angiotensin II-induced activation of the SHP-2 tyrosine phosphatase. *J Cell Physiol*. 2005;205:402–413.
- Weber DS, Taniyama Y, Rocic P, Seshiah PN, Dechert MA, Gerthoffer WT, Griendling KK. Phosphoinositide-dependent kinase 1 and p21-activated protein kinase mediate reactive oxygen species-dependent regulation of platelet-derived growth factor-induced smooth muscle cell migration. *Circ Res*. 2004;94:1219–1226.
- Beier I, Düsing R, Vetter H, Schmitz U. Epidermal growth factor stimulates Rac1 and p21-activated kinase in vascular smooth muscle cells. *Atherosclerosis*. 2008;196:92–97.
- Kumar R, Gururaj AE, Barnes CJ. p21-activated kinases in cancer. *Nat Rev Cancer*. 2006;6:459–471.
- Gregg D, Rauscher FM, Goldschmidt-Clermont PJ. Rac regulates cardiovascular superoxide through diverse molecular interactions: more than a binary GTP switch. *Am J Physiol Cell Physiol*. 2003;285:C723–C734.
- Noma K, Oyama N, Liao JK. Physiological role of ROCKs in the cardiovascular system. *Am J Physiol Cell Physiol*. 2006;290:C661–C668.
- Cai X, Wu JH, Exum ST, Oppermann M, Premont RT, Shenoy SK, Freedman NJ. Reciprocal regulation of the platelet-derived growth factor receptor-beta and G protein-coupled receptor kinase 5 by cross-phosphorylation: effects on catalysis. *Mol Pharmacol*. 2009;75:626–636.
- Penzes P, Johnson RC, Alam MR, Kambampati V, Mains RE, Eipper BA. An isoform of kalirin, a brain-specific GDP/GTP exchange factor, is enriched in the postsynaptic density fraction. *J Biol Chem*. 2000;275:6395–6403.
- McPherson CE, Eipper BA, Mains RE. Multiple novel isoforms of Trio are expressed in the developing rat brain. *Gene*. 2005;347:125–135.
- Kim J, Zhang L, Peppel K, Wu JH, Zidar DA, Brian L, DeWire SM, Exum ST, Lefkowitz RJ, Freedman NJ. Beta-arrestins regulate atherosclerosis and neointimal hyperplasia by controlling smooth muscle cell proliferation and migration. *Circ Res*. 2008;103:70–79.
- Nakashima Y, Plump AS, Raines EW, Breslow JL, Ross R. ApoE-deficient mice develop lesions of all phases of atherosclerosis throughout the arterial tree. *Arterioscler Thromb*. 1994;14:133–140.
- Ferraro F, Ma XM, Sobota JA, Eipper BA, Mains RE. Kalirin/Trio Rho guanine nucleotide exchange factors regulate a novel step in secretory granule maturation. *Mol Biol Cell*. 2007;18:4813–4825.
- Bokoch GM. Biology of the p21-activated kinases. *Annu Rev Biochem*. 2003;72:743–781.
- Yoneda A, Mulhaupt HA, Couchman JR. The Rho kinases I and II regulate different aspects of myosin II activity. *J Cell Biol*. 2005;170:443–453.
- Wheeler AP, Ridley AJ. Why three Rho proteins? RhoA, RhoB, RhoC, and cell motility. *Exp Cell Res*. 2004;301:43–49.
- Bouquier N, Vignal E, Charrasse S, Weill M, Schmidt S, Léonetti JP, Blangy A, Fort P. A cell active chemical GEF inhibitor selectively targets the Trio/RhoG/Rac1 signaling pathway. *Chem Biol*. 2009;16:657–666.
- Ferri N, Corsini A, Bottino P, Clerici F, Contini A. Virtual screening approach for the identification of new Rac1 inhibitors. *J Med Chem*. 2009;52:4087–4090.
- Michaelson D, Abidi W, Guardavaccaro D, Zhou M, Ahearn I, Pagano M, Philips MR. Rac1 accumulates in the nucleus during the G2 phase of the cell cycle and promotes cell division. *J Cell Biol*. 2008;181:485–496.
- Noma K, Rikitake Y, Oyama N, Yan G, Alcaide P, Liu PY, Wang H, Ahl D, Sawada N, Okamoto R, Hiroi Y, Shimizu K, Lusinskas FW, Sun J, Liao JK. ROCK1 mediates leukocyte recruitment and neointima formation following vascular injury. *J Clin Invest*. 2008;118:1632–1644.
- Penzes P, Beeser A, Chernoff J, Schiller MR, Eipper BA, Mains RE, Huganir RL. Rapid induction of dendritic spine morphogenesis by trans-synaptic ephrinB-EphB receptor activation of the Rho-GEF kalirin. *Neuron*. 2003;37:263–274.
- Foo SS, Turner CJ, Adams S, Compagni A, Aubyn D, Kogata N, Lindblom P, Shani M, Zicha D, Adams RH. Ephrin-B2 controls cell motility and adhesion during blood-vessel-wall assembly. *Cell*. 2006;124:161–173.
- Simon DI, Dhen Z, Seifert P, Edelman ER, Ballantyne CM, Rogers C. Decreased neointimal formation in Mac-1(-/-) mice reveals a role for inflammation in vascular repair after angioplasty. *J Clin Invest*. 2000;105:293–300.
- Yan Z, Hansson GK. Overexpression of inducible nitric oxide synthase by neointimal smooth muscle cells. *Circ Res*. 1998;82:21–29.
- Moore ZW, Hui DY. Apolipoprotein E inhibition of vascular hyperplasia and neointima formation requires inducible nitric oxide synthase. *J Lipid Res*. 2005;46:2083–2090.
- Zhang L, Peppel K, Sivashanmugam P, Orman ES, Brian L, Exum ST, Freedman NJ. Expression of tumor necrosis factor receptor-1 in arterial wall cells promotes atherosclerosis. *Arterioscler Thromb Vasc Biol*. 2007;27:1087–1094.

Arteriosclerosis, Thrombosis, and Vascular Biology



JOURNAL OF THE AMERICAN HEART ASSOCIATION

Kalirin Promotes Neointimal Hyperplasia by Activating Rac in Smooth Muscle Cells

Jiao-Hui Wu, Alexander C. Fanaroff, Krishn C. Sharma, Liisa S. Smith, Leigh Brian, Betty A. Eipper, Richard E. Mains, Neil J. Freedman and Lisheng Zhang

Arterioscler Thromb Vasc Biol. published online January 3, 2013;

Arteriosclerosis, Thrombosis, and Vascular Biology is published by the American Heart Association, 7272 Greenville Avenue, Dallas, TX 75231

Copyright © 2013 American Heart Association, Inc. All rights reserved.

Print ISSN: 1079-5642. Online ISSN: 1524-4636

The online version of this article, along with updated information and services, is located on the World Wide Web at:

<http://atvb.ahajournals.org/content/early/2013/01/03/ATVBAHA.112.300234>

Data Supplement (unedited) at:

<http://atvb.ahajournals.org/content/suppl/2013/01/03/ATVBAHA.112.300234.DC1>

Permissions: Requests for permissions to reproduce figures, tables, or portions of articles originally published in *Arteriosclerosis, Thrombosis, and Vascular Biology* can be obtained via RightsLink, a service of the Copyright Clearance Center, not the Editorial Office. Once the online version of the published article for which permission is being requested is located, click Request Permissions in the middle column of the Web page under Services. Further information about this process is available in the [Permissions and Rights Question and Answer](#) document.

Reprints: Information about reprints can be found online at:

<http://www.lww.com/reprints>

Subscriptions: Information about subscribing to *Arteriosclerosis, Thrombosis, and Vascular Biology* is online at:

<http://atvb.ahajournals.org/subscriptions/>

SUPPLEMENTAL MATERIAL

Expanded Methods

Materials

The Kalirin RhoGEF1-selective inhibitor NPPD (1-(3-nitrophenyl)-1*H*-pyrrole-2,5-dione) was obtained from Chembridge, Inc. The Kalirin RhoGEF1-selective inhibitor ITX3 (2-[(2,5-Dimethyl-1-phenyl-1*H*-pyrrol-3-yl)methylene]-thiazolo[3,2-*a*]benzimidazol-3(2*H*)-one) was obtained from Sigma-Aldrich, Inc. The Rac1 inhibitor Z62954982 (3-((3,5-Dimethylisoxazol-4-yl)methoxy)-*N*-(4-methyl-3-sulfamoyl-phenyl)benzamide) was obtained from EMD Millipore. Cell culture supplies were from Invitrogen, unless specified otherwise. Human PDGF-BB was from Millipore.

Antibodies against the following proteins were from the following sources: phospho- (p-)Thr423-PAK (sc-12925), total PAK1 (sc-881), PLC- γ 1 (sc-7290), actin c-19 (sc-1616), PDGFR β (sc-432), RhoA (clone 26C4, sc-418), and β -Tubulin (sc-9104) were all from Santa Cruz Biotechnology; p-Thr853-MYPT1 (rabbit polyclonal, #4563) and p-ERK1/2 (clone E10) were from Cell Signaling, Inc.; MYPT1 (07-672) and Rac1 (clone 23A8) were from Millipore; endothelin receptor subtype A (ET_A-R) was from Alomone Labs, Inc.; SMC-actin (clone 1A4, conjugated to Cy-3), PCNA (clone PC10), and collagen I (clone COL-1) were obtained from Sigma-Aldrich; CD11b (clone M1/70) and isotype control IgG conjugated to phycoerythrin were obtained from BioLegend, Inc.; von Willebrand factor (vWF) was obtained from DakoCytomation (rabbit polyclonal #A0082); GRK5 (clone A16/17) was produced as described.¹ Polyclonal rabbit antisera specific for the Kalirin spectrin domain (spectrin-like repeats 4-7)² or Trio³ were produced as described.

Mice

All mice were congenic (≥ 10 generations back-crossed) on the C57BL/6 background. *Kalrn*^{flox/+} mice harbored a *Kalrn* allele containing loxP sites flanking exon 13 (of the spectrin repeat domain); they were produced as described, and crossed with FLPeR mice to remove the neomycin resistance cassette.⁴ It is important to note that knockout of *Kalrn* exon 13 prevents the synthesis of all Kalirin isoforms except the minor species known as delta-Kalirin-9 and Duet.⁴ These mice were crossed with CMV-Cre-transgenic mice (Jackson Labs, stock #006054) to obtain *Kalrn*^{-/+} mice, which were then bred to eliminate the CMV-Cre transgene. *Kalrn*^{flox/+} mice were crossed with SM22 α -Cre-transgenic mice (Jackson Labs, stock #004746) to obtain mice with SMC-specific *Kalrn* deficiency (SM22 α -Cre⁺/*Kalrn*^{flox/+}, or SMC-*Kalrn*^{-/+}). *Kalrn*^{-/-} and littermate WT mice were obtained from crosses of *Kalrn*^{-/+} mice. *Apoe*^{-/-} mice were from Jackson Labs. All mutant mice were back-crossed to C57BL/6J WT (Jackson Labs, stock #000664) every 5 generations, to minimize genetic drift. All animal experiments complied with Duke University Institutional Animal Care and Use Committee guidelines.

Blood pressure was measured by tail cuff plethysmography with a MC4000 Blood Pressure Analysis System (Hatteras Instruments). After 10 days' training, mice were subjected to 10 consecutive days of measurements; a single day's measurements constituted the mean of 10 determinations made on each mouse. Hemodynamic measurements were made by an investigator unaware of mouse genotypes.

Cell Culture

Mouse aortic SMCs were isolated by enzymatic digestion of aortas and passaged as we have described.⁵ Mouse aortas were stripped of adventitia and endothelial cells, and then digested at 37 °C for 1.5 h in PBS containing the following reagents (all from Sigma): collagenase II (1 mg/ml), elastase type III (0.125 mg/ml), soybean trypsin inhibitor (0.375 mg/ml), and bovine serum albumin (fraction V, 2 mg/ml) in DMEM. Released SMCs were cultured in DMEM with 20% FBS, 1% anti-mycotic/antibiotic (Invitrogen) and 1% Mycoplasma Removal Agent (MP Biomedicals) for one wk, and then in DMEM with 10% FBS, 1% penicillin/streptomycin thereafter. SMCs were split at 1:4, and used during passages

3–7. These primary SMCs demonstrated >95% prevalence of SMC α -actin expression by immunofluorescence.

Endothelial cells were isolated from mouse aortas and cultured exactly as described.⁵ Macrophages were differentiated from bone marrow precursors with colony-stimulating factor-1, exactly as described.⁵

Immunoblotting

Tissues were snap-frozen in liquid nitrogen, pulverized with a mortar and pestle, and then solubilized in SDS sample buffer or Buffer A: 50 mmol/L Tris-Cl (pH 8 at 25 °C); 1% (w/v) Triton-X-100; 0.05% (w/v) SDS; 200 mmol/L NaCl; 50 mmol/L NaF (Ser/Thr phosphatase inhibitor); 10 mmol/L disodium pyrophosphate (Ser/Thr phosphatase inhibitor); plus protease inhibitors.⁶ Cells were solubilized in either SDS sample buffer (followed by sonication) or in Buffer A. After solubilization, samples were centrifuged ($10,000 \times g$, 10 min, 4 °C) to remove insoluble debris. Protein was quantitated in samples solubilized in Buffer A with a modified Lowry assay (BioRad), and equal protein masses were loaded in each lane for SDS-PAGE, which was performed on 4–12% polyacrylamide gradient gels or 10% polyacrylamide gels (Invitrogen). Semi-dry transfer, immunoblotting and chemiluminescent detection were performed as described.⁶ Band density was quantitated by NIH Image J.

SMC Assays

Proliferation and migration assays were performed on serum-starved SMCs as we described.^{7,8} For signaling assays, SMCs were incubated overnight (37 °C, 16 hr) in 30-mm dishes in serum-free medium (Dulbecco's modified Eagle Medium [Invitrogen], 20 mmol/L Hepes pH 7.4, 1 mg/ml of fatty acid-free bovine serum albumin [Sigma], 100 units/ml penicillin, and 100 μ g/ml streptomycin [Invitrogen]). SMCs were then stimulated for the indicated times with either 10% (vol/vol) fetal bovine serum or the indicated concentration of PDGF-BB, and then lysed in ice-cold Buffer A (above).

Quantitation of RhoA-GTP and Rac1-GTP was performed with G-LISAs (Cytoskeleton, Inc.), according to the manufacturer's instructions.

Carotid Endothelial Denudation

These studies were performed as we described previously,⁹ with a 0.36-mm-diameter coronary guidewire (Cordis) using a modification of the method of Lindner et al.¹⁰ We used 8-wk-old WT, *Kalrn*^{+/+}, and SMC-*Kalrn*^{+/+} mice matched for gender and pre-operative weight (21 ± 3 grams). Mice were anesthetized with pentobarbital (50 mg/kg). We created a midline neck incision extending from the lower mandible to the sternum, and then loosely tied 10-0 "control sutures" at the proximal portion of the common and internal carotid arteries and at the mid-portion of the external carotid artery, to prevent blood flow without engendering arterial wall damage. We next extended a ~0.5 mm external carotid arteriotomy from the control suture to the carotid artery bifurcation, and flushed the common carotid with PBS. To denude the endothelium, we traversed the length of the common carotid three times with a 0.36-mm flexible angioplasty guidewire (Johnson and Johnson). After removing the wire, we ligated the external carotid artery proximally after flushing the common carotid with blood, and then completely released the control sutures. Mice were sacrificed 4 wk post-operatively. At the time of sacrifice, mouse weights were equivalent in each distinct genetic group. There were no carotid thromboses in this series of mice; the overall thrombosis rate for this procedure in our hands is <2%.

Histology/Immunofluorescence Microscopy

Immunofluorescence was performed on OCT-embedded carotid arteries cut at 5- μ m, as described.¹¹ The DNA-binding fluorophore Hoechst 33342 (10 μ g/ml) was added to secondary antibody incubations. To minimize elastic laminae fluorescence, we used 0.2% gelatin in both blocking and IgG diluent buffer: 20 mmol/L Tris-Cl (pH 7.5)/125 mmol/L NaCl/ 0.1% (vol/vol) Tween-20. Single microscopic fields were imaged for multiple fluorophores, and protein immunofluorescence was quantitated by normalizing to nuclear DNA fluorescence (as a measure of cellularity), exactly as described.¹¹ All specimens stained within a single batch were imaged with identical CCD camera and microscope settings. In all cases,

nonspecific fluorescence (with non-immune primary IgG) was subtracted from total fluorescence, to obtain antigen-specific fluorescence. Immunofluorescence was quantitated by observers blinded to specimen identity.

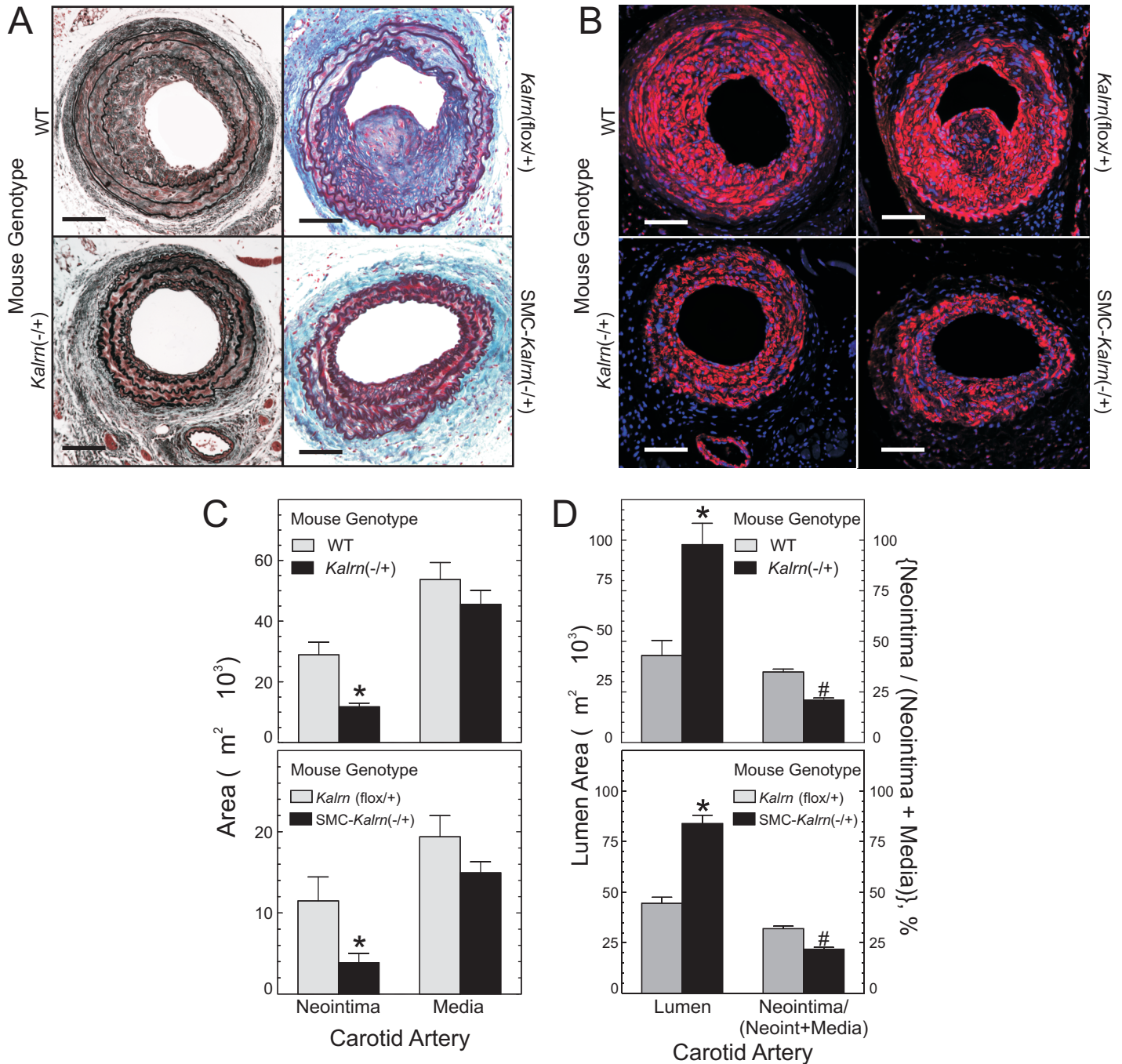
Perfusion-fixed specimens were paraffin-embedded, sliced and stained with a modified Masson's trichrome and Verhoeff's elastic tissue stain as we previously described.^{5,9,12-14} Planimetry was performed with NIH Image J by observers blinded to specimen identity, as we described.^{5,9,12-14}

Statistical Analyses

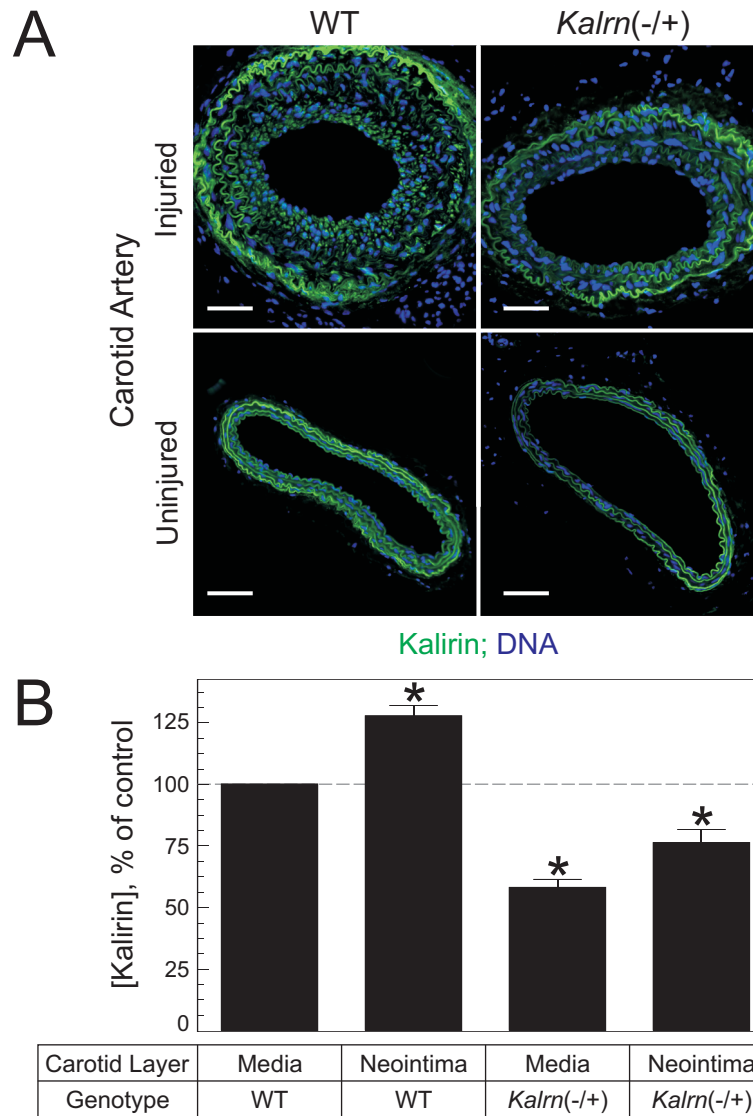
Data are presented as mean \pm S.D. in the text and as mean \pm S.E. in the figures. Data from experiments with only two independent means were analyzed by *t* tests. Data from experiments with multiple groups were compared by one-way ANOVA with Tukey's post-hoc test for multiple comparisons. Time course analyses were performed by two-way ANOVA, and SMC migration data were analyzed by repeated measures two-way ANOVA with a Bonferroni post-hoc test. Statistical software was Prism[®] 5 (GraphPad, Inc.).

Supplemental References

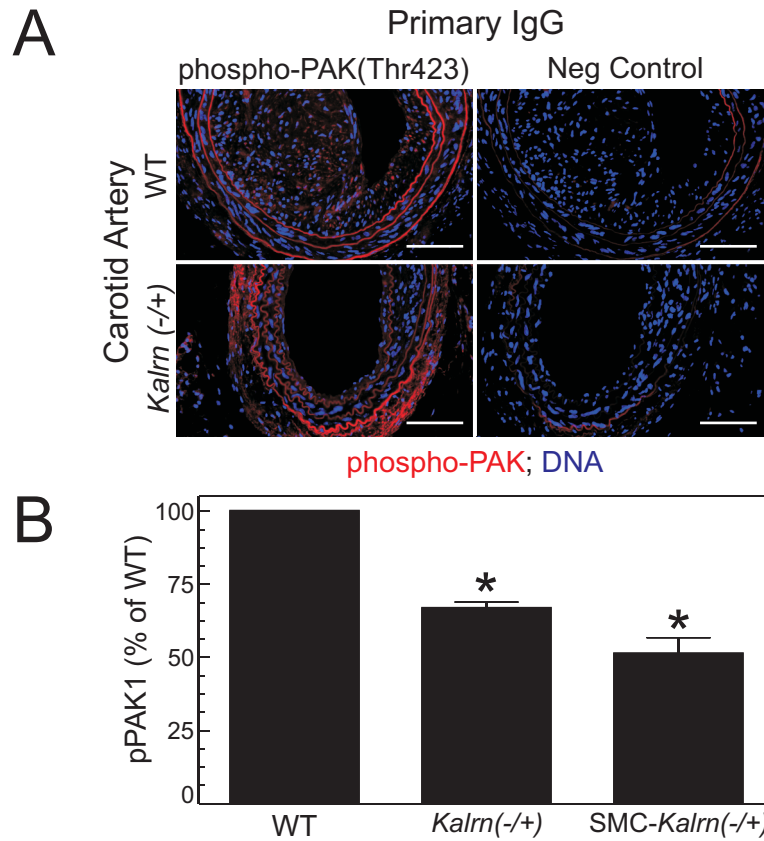
1. Oppermann M, Diverse-Pierluissi M, Drazner MH, Dyer SL, Freedman NJ, Peppel KC, Lefkowitz RJ. Monoclonal antibodies reveal receptor specificity among G-protein-coupled receptor kinases. *Proc Natl Acad Sci USA*. 1996;93:7649-7654.
2. Penzes P, Johnson RC, Alam MR, Kambampati V, Mains RE, Eipper BA. An isoform of kalirin, a brain-specific GDP/GTP exchange factor, is enriched in the postsynaptic density fraction. *J Biol Chem*. 2000;275:6395-6403.
3. McPherson CE, Eipper BA, Mains RE. Genomic organization and differential expression of Kalirin isoforms. *Gene*. 2002;284:41-51.
4. Mandela P, Yankova M, Conti LH, Ma X, Grady J, Eipper BA, Mains RE. Kalrn plays key roles within and outside of the nervous system *BMC Neurosci*. 2012;13:136 (in press).
5. Wu JH, Zhang L, Fanaroff AC, Cai X, Sharma KC, Brian L, Exum ST, Shenoy SK, Peppel K, Freedman NJ. G Protein-coupled Receptor Kinase-5 Attenuates Atherosclerosis by Regulating Receptor Tyrosine Kinases and 7-transmembrane Receptors. *Arterioscler Thromb Vasc Biol*. 2012;32:308-316.
6. Freedman NJ, Ament AS, Oppermann M, Stoffel RH, Exum ST, Lefkowitz RJ. Phosphorylation and desensitization of human endothelin A and B receptors: evidence for G protein-coupled receptor kinase specificity. *J Biol Chem*. 1997;272:17734-17743.
7. Zhang L, Sivashanmugam P, Wu JH, Brian L, Exum ST, Freedman NJ, Peppel K. Tumor necrosis factor receptor-2 signaling attenuates vein graft neointima formation by promoting endothelial recovery. *Arterioscler Thromb Vasc Biol*. 2008;28:284-289.
8. Wu JH, Goswami R, Cai X, Exum ST, Huang X, Zhang L, Brian L, Premont RT, Peppel K, Freedman NJ. Regulation of the platelet-derived growth factor receptor- β by G protein-coupled receptor kinase-5 in vascular smooth muscle cells involves the phosphatase Shp2. *J Biol Chem*. 2006;281:37758-37772.
9. Kim J, Zhang L, Peppel K, Wu JH, Zidar DA, Brian L, DeWire SM, Exum ST, Lefkowitz RJ, Freedman NJ. β -arrestins regulate atherosclerosis and neointimal hyperplasia by controlling smooth muscle cell proliferation and migration. *Circ Res*. 2008;103:70-79.
10. Lindner V, Fingerle J, Reidy MA. Mouse model of arterial injury. *Circ Res*. 1993;73:792-796.
11. Zhang L, Peppel K, Brian L, Chien L, Freedman NJ. Vein graft neointimal hyperplasia is exacerbated by tumor necrosis factor receptor-1 signaling in graft-intrinsic cells. *Arterioscler Thromb Vasc Biol*. 2004;24:2277-2283.
12. Zhang L, Peppel K, Sivashanmugam P, Orman ES, Brian L, Exum ST, Freedman NJ. Expression of tumor necrosis factor receptor-1 in arterial wall cells promotes atherosclerosis. *Arterioscler Thromb Vasc Biol*. 2007;27:1087-1094.
13. Shah SH, Freedman NJ, Zhang L, et al. Neuropeptide Y gene polymorphisms confer risk of early-onset atherosclerosis. *PLoS Genet*. 2009;5:e1000318 (1000311-1000310).
14. Zhang L, Connelly JJ, Peppel K, et al. Aging-related atherosclerosis is exacerbated by arterial expression of tumor necrosis factor receptor-1: evidence from mouse models and human association studies. *Hum Mol Genet*. 2010;19:2754-2766.
15. Kumar R, Gururaj AE, Barnes CJ. p21-activated kinases in cancer. *Nat Rev Cancer*. 2006;6:459-471.



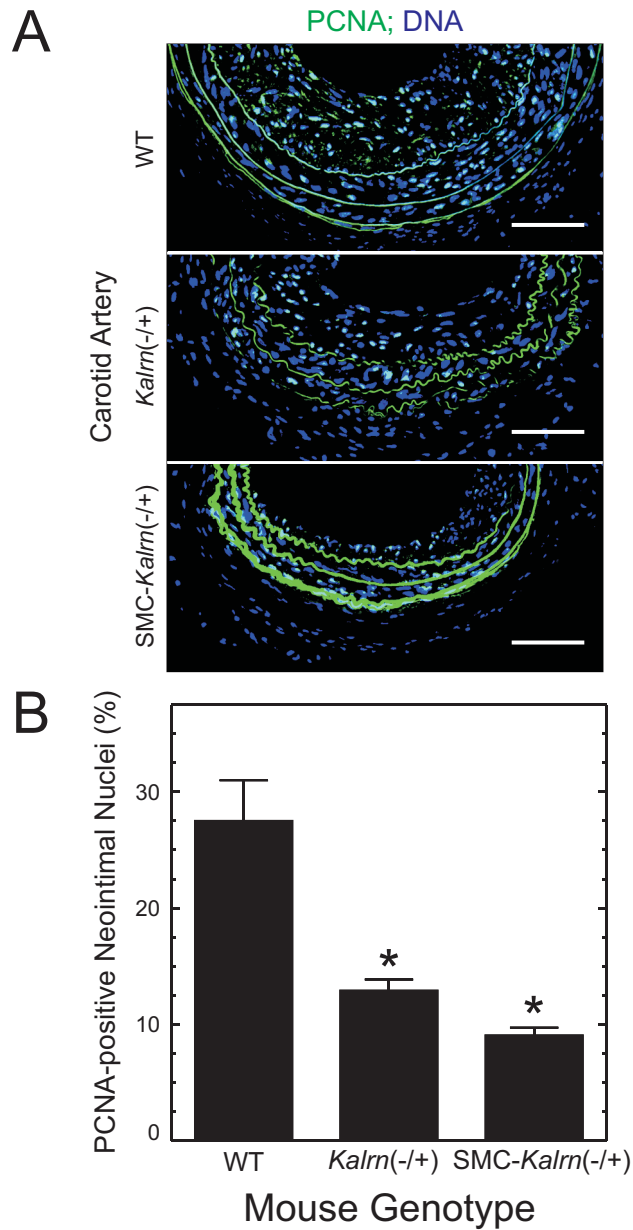
Supplemental Figure I. SMC Kalirin promotes neointimal hyperplasia (an expanded version of Figure 6). **A**, Figure 6B has been rendered in color here. Scale bar = 50 μm . **B**, Serial sections from Panel A were stained for SMC actin (red) and DNA (blue). Although SMC actin staining is variable as one would expect in samples with varying degrees of SMC activation and proliferation, all neointimal cells demonstrate SMC actin immunoreactivity. Specimens shown represent at least 5 independent specimens of each genotype. **C**, Figure 6C has been re-formatted here, for comparison with Panel D. Compared with WT: *, $p < 0.02$. **D**, The indicated carotid artery dimension is plotted as means \pm S.E. from at least 5 carotids of each genotype. Compared with WT: *, $p < 0.01$; #, $p < 0.05$.



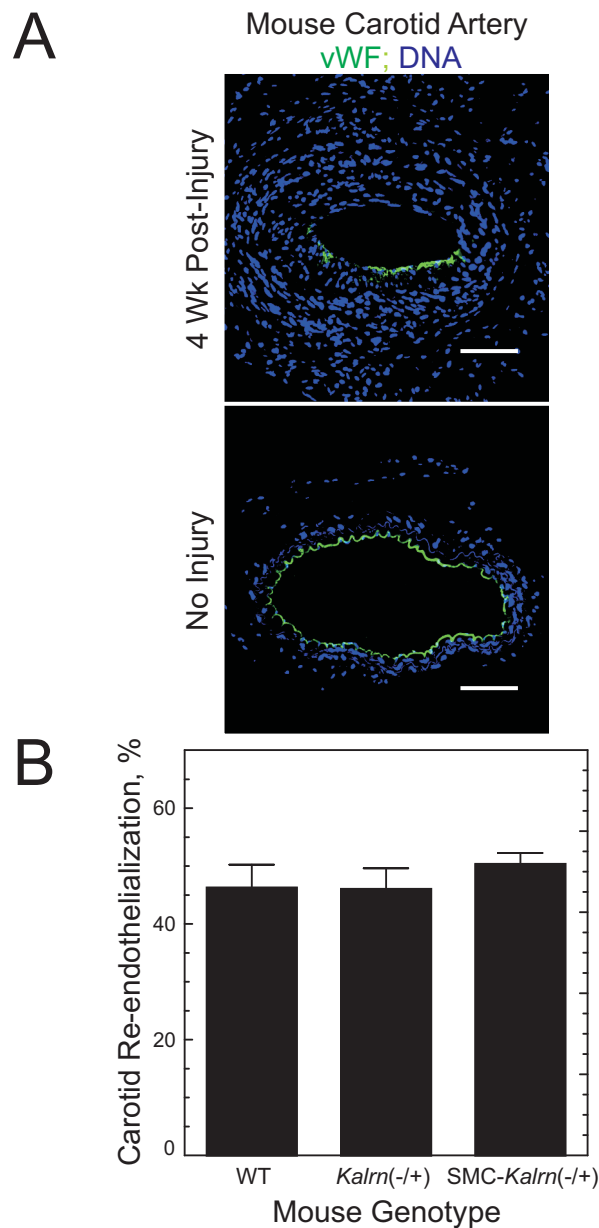
Supplemental Figure II. Kalirin up-regulates during neointimal hyperplasia. **A**, Carotid arteries from the cohort used in Figure 6, as well as contralateral uninjured carotids, were stained with rabbit IgG specific for Kalrin isoforms 7, 9, and 12, or with non-immune control rabbit IgG. Secondary incubations were with Alexa-488-conjugated anti-rabbit IgG (green) and Hoechst 33342 (DNA, blue). Scale bars = 50 μ m (original magnification \times 220). Shown are samples of the indicated genotype, all stained in the same batch, representative of four such sample groups. Specimens stained with non-immune rabbit IgG showed elastin autofluorescence, but no green immunofluorescence (not shown). **B**, Within each immunostaining group, the ratios of Kalirin immunofluorescence to DNA fluorescence intensity within the medias and neointimas were normalized to those obtained from the media of the injured WT sample(s), to yield “% of control.” Plotted are the means \pm S.E. of 4 specimens of each group. Compared with Kalirin immunofluorescence in the media of WT samples: *, $p < 0.05$.



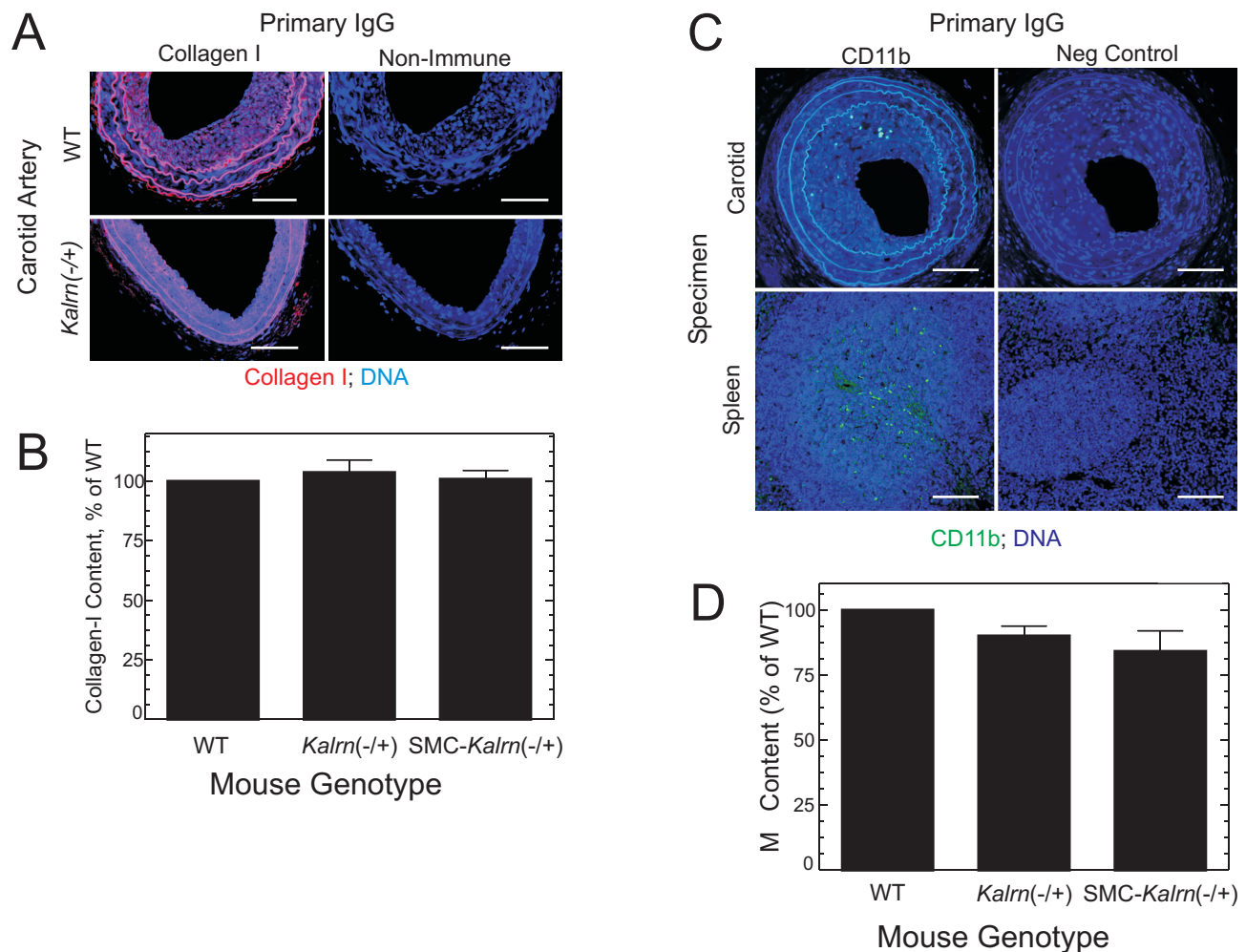
Supplemental Figure III. Kalirin promotes activation of PAK in neointimal hyperplasia. **A**, Serial sections of specimens from Figure 6 were stained with IgG specific for phospho-Thr423-PAK (pPAK, red) and DNA (Hoechst 33342, blue). Scale bars = 50 μ m (original magnification \times 220). **B**, Neointimal phospho-PAK immunofluorescence was normalized to DNA fluorescence intensity; the resulting ratios were normalized to those of WT specimens stained in the same batch, to yield “% of WT.” The resulting ratios in each group are graphed as the means \pm S.E. of 4 specimens of each group. Compared with injured WT carotid samples: *, $p < 0.01$.



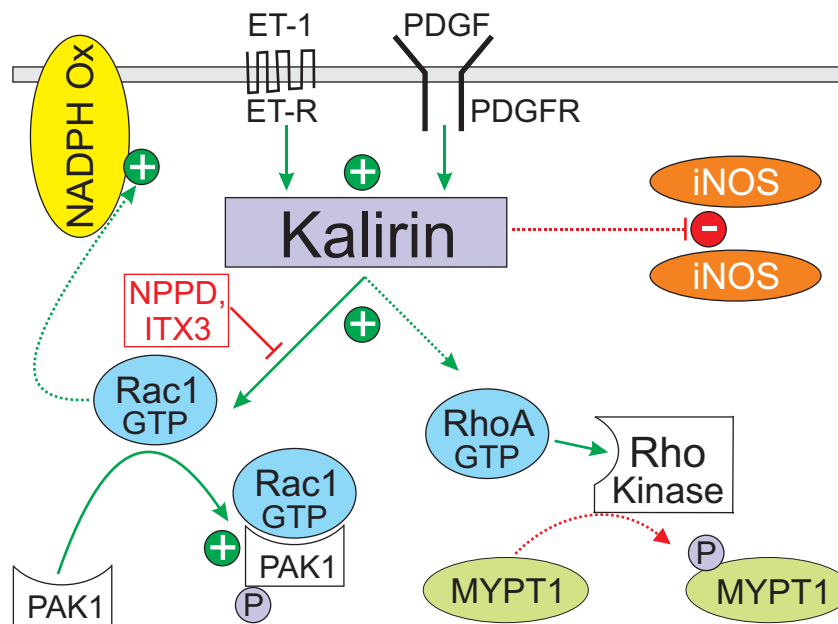
Supplemental Figure IV. Kalirin promotes SMC proliferation in neointimal hyperplasia. **A**, Serial sections of specimens from Figure 6 were stained for proliferating cell nuclear antigen (PCNA, green) and DNA (Hoechst 33342, blue). Shown are individual samples, representative of 4 from each genotype. Scale bars = 50 μ m (original magnification $\times 220$). **B**, The number of PCNA-positive nuclei in the neointima of each specimen was normalized to the total number of neointimal nuclei, to obtain “% PCNA-positive.” Plotted are the means \pm S.E. of 4 specimens from each group. Compared with injured WT carotid samples: *, $p < 0.01$.



Supplemental Figure V. Kalirin does not affect re-endothelialization of wire-injured carotid arteries. **A**, Serial sections of specimens from Figure 6, along with uninjured negative control carotid sections, were stained for von Willebrand factor (vWF, green) and DNA (Hoechst 33342, blue). Shown are individual samples, representative of 4 from each genotype. Scale bars = 50 μ m (original magnification $\times 220$). **B**, The percentage of luminal surface that stained for vWF was averaged across samples within the same genetic group, to obtain “% Re-endothelialization.” Plotted are the means \pm S.E. of 4 specimens from each group.



Supplemental Figure VI. Kalirin does not affect neointimal collagen or macrophage content after carotid artery endothelial denudation. **A**, Serial sections of specimens from Figure 6 were stained for collagen I (red) and DNA (Hoechst 33342, blue). Scale bar = 50 μ m (original magnification $\times 220$). **B**, Neointimal collagen immunofluorescence was normalized to DNA fluorescence intensity; the resulting ratios were divided by those of WT specimens in the same staining batch, to yield “% of WT.” Plotted are the means \pm S.E. of 4 specimens from each genetic group. **C**, Serial sections of specimens from Figure 6, along with paraffin-embedded mouse spleen, were stained with anti-CD11b or isotype control IgG (green), and Hoechst 33342 (DNA, blue). Scale bar = 50 μ m (original magnification $\times 220$). In the neointima and media, macrophage (M) immunofluorescence was normalized to DNA fluorescence; the resulting ratios were divided by those of WT in the same staining batch, to yield “% of WT.” Plotted are the means \pm S.E. of 4 specimens from each genetic group.



Supplemental Figure VII. Kalirin-mediated signal transduction in SMCs. Kalirin is activated downstream of the receptor tyrosine kinase for PDGF (PDGFR in SMCs) or the Gq-coupled, 7-transmembrane endothelin (ET) receptors. Kalirin's RhoGEF1 activates Rac1 in SMCs; no evidence yet suggests that Kalirin's RhoGEF2 can activate RhoA in SMCs as it can in neurons. Kalirin's Rho-GEF1 is inhibited by NPPD (1-(3-nitro-phenyl)-1*H*-pyrrole-2,5-dione) or ITX3 (2-[(2,5-Dimethyl-1-phenyl-1*H*-pyrrol-3-yl)methylene]-thiazolo[3,2-*a*]benzimidazol-3(2*H*)-one). Signaling to p21-activated kinase (*PAK*) can engender SMC proliferation by *PAK*-mediated phosphorylation of MEK and RAF1 (leading to ERK activation), phosphorylation of the p47^{phox} subunit of NADPH oxidase (increasing NADPH oxidase activation), and activation of NF κ B-inducing kinase (activating NF κ B), among other mechanisms.¹⁵ Potential effects of Kalirin on Rho kinase, NADPH oxidase and inducible NO synthase (iNOS) are illustrated. Green, stimulation; red, inhibition; dotted lines, not yet demonstrated downstream of Kalirin in SMCs.